

ON APPLICATION OF RATIONAL DISCRETE SHORT TIME FOURIER TRANSFORM IN EPILEPTIC SEIZURE CLASSIFICATION

Péter Kovács^a, Kaveh Samiee^b, Moncef Gabbouj^b

^a Eötvös L. University, Budapest, Hungary,

^b Tampere University of Technology, Tampere, Finland

ABSTRACT

This work deals with an adaptive and localized time-frequency representation of time-series signals based on rational functions. The proposed rational Discrete Short Time Fourier Transform (DSTFT) is used for extracting discriminative features in EEG data. We take the advantages of bagging ensemble learning and Alternating Decision Tree (ADTree) classifier to detect the seizure segments in presence of seizure-free segments. The effectiveness of different rational systems is compared with the classical Short Time Fourier Transform (STFT). The comparative study demonstrates that Malmquist–Takenaka rational system outperforms STFT while it can provide a tunable time-frequency representation of the EEG signals and less Mean Square Error (MSE) in the inverse transform.

Index Terms— EEG time series, seizure classification, rational functions, Malmquist–Takenaka system.

1. INTRODUCTION

In the last decade, a wide range of signal processing and machine learning algorithms have been adapted to be employed in seizure detection and EEG classification. In general, achieving discriminative features, in the time and/or frequency domains, which can describe epileptic seizure patterns, is the most important part of the epileptic seizure detection. Continuous and discrete Wavelet transform provide a simultaneous representation in time/frequency domains which is a powerful tool for analysis of non-stationary EEG signal. Wavelet based methods are mostly used to decompose the EEG signal into frequency sub-bands. As an alternate and a special case to Short Time Fourier transform (STFT), Gabor transform has been employed in epileptic seizure analysis. In [1], the usage of Gabor transform and Frequency Band Relative Intensity Ratio (FBRIR) are explored in describing the EEG signal patterns during ictal epileptic discharge. A filter bank consisting of a number of Gabor filters, with different parameters such as orientations and central frequencies, was

The research was supported by the National Development Agency (NFÜ), Hungary (grant agreement Research and Technology Innovation Fund. EITKIC_12.)

used to detect the seizure and non-seizure epochs in a system which takes the advantages of both scalp EEG and electrocardiography (ECG) to improve the information extraction [2].

The rational functions were efficiently used to represent one period of an electrocardiograph [3, 4]. Furthermore, these systems were successfully applied for modeling the QRS complex [5] and for compressing the heart beats as well. In the present work, we are taking advantage of the former experience on ECG signals and we propose an EEG model based on rational functions. Additionally, we use the rational system as a competitive to STFT for representation of the EEG signal in time-frequency domain. Finally, we provide a feature extraction technique for seizure classification.

2. RATIONAL FUNCTIONS

In this section we give a brief introduction about the theory of rational functions. So let \mathbb{C} stand for the set of complex numbers, $\mathbb{D} := \{z \in \mathbb{C} : |z| < 1\}$ for the open unit disc, $\mathbb{N} := \{1, 2, 3, \dots\}$ for the set of natural numbers, and $\mathbb{T} := \{z \in \mathbb{C} : |z| = 1\}$ for the unit circle (or torus).

Consider the series with different elements $a_0, \dots, a_n \in \mathbb{D}$ and the sequence $m_0, \dots, m_n \in \mathbb{N}$ called poles and multiplicities. Then, the modified rational functions (MRF) are defined as follows

$$\varphi_{k,i}(z) = \frac{z^{i-1}}{(1 - \bar{a}_k z)^i} \quad (k = 0, \dots, n, i = 1, \dots, m_k).$$

The parameter a_k is referred to as *inverse pole* (because $1/\bar{a}_k$ is a pole in the standard sense), i is said to be the *order* of the basic function. Using a terminology similar to the trigonometric case, the value $i = 1$ corresponds to the *fundamental tone* and $i > 1$ the *overtone*s.

The corresponding biorthogonal rational functions [6] and the so-called Malmquist–Takenaka (MT) system [7] are

$$\Psi_{k,i}(z) = \frac{\Omega_{kn}(z)(z - a_k)^{i-1}}{\Omega_{kn}(a_k)} \sum_{s=0}^{m_k-i} \frac{\omega_{kn}^{(s)}(a_k)}{s!} (z - a_k)^s,$$

$$\Phi_k(z) = \frac{\sqrt{1 - |a_k|^2}}{1 - \bar{a}_k z} \prod_{j=0}^{k-1} \frac{z - a_j}{1 - \bar{a}_j z}, \quad (z \in \mathbb{C} \setminus \{1/\bar{a}_j\}),$$

where

$$\Omega_{kn}(z) = \frac{1}{(1 - \bar{a}_k z)^{m_k}} \prod_{i=0, i \neq k}^n \left(\frac{z - a_i}{1 - \bar{a}_i z} \right)^{m_i},$$

$$\omega_{kn}(z) = \frac{\Omega_{kn}(a_k)}{\Omega_{kn}(z)},$$

with $0 \leq k \leq n$ and $1 \leq i \leq m_k$. The systems above are biorthogonal and orthogonal with respect to the scalar product of the Hardy space $\langle F, G \rangle = \frac{1}{2\pi} \int_{-\pi}^{\pi} F(e^{it}) \overline{G(e^{it})} dt$ for $F, G \in H^2(\mathbb{D})$. Additionally, we note that the MT and the biorthogonal systems Φ and Ψ with the modified rational functions φ are referred as the rational orthogonal basis (ROB) in the literature (see e.g., Heuberger et al. [7]).

3. GENERALIZED SHORT TIME FOURIER TRANSFORM

Fourier transform is a well-known tool for analyzing the frequency distribution of a signal. Unfortunately, the time information has been lost during this transformation. On the other hand, several techniques like short time Fourier transform (STFT), Cohen's class distributions, Wavelets, etc. are attempted to solve this problem.

Let us denote the uniformly sampled $f(t)$ and $g(t)$ functions by $f[n]$ and $g[n]$. Then the discrete (D) STFT over a compactly supported g window function can be written as

$$\mathcal{F}_g f[n, k] = \sum_{m=0}^{M-1} f[n-m] g[m] \epsilon_k[m], \quad (1)$$

where $\epsilon_k[m] = e^{-2\pi m \frac{k}{N}}$, M is the window length of g and N is the number of samples in f . This algorithm can be interpreted as a successive evaluation of Fourier transforms over short segments of the whole signal. Additionally, the frequencies can be visually represented by displaying the squared magnitude of the Fourier coefficients at each section. This diagram is called as the spectrogram of the signal f .

Using the same terminology as in Eq. (1) we can define a similar representation of the signal by replacing the trigonometric bases ϵ_k with the elements of the ROB. More precisely, let us consider a single pole a_0 with multiplicity $m_0 = M$, and an $f \in H^2(\mathbb{D})$ uniformly sampled function. Then the generalized rational DSTFT can be written as

$$\mathcal{R}_\phi \mathcal{F}_g f[n, k] = \sum_{m=0}^{M-1} f[n-m] g[m] \phi_k[m], \quad (2)$$

where $\phi_k[m] = \Phi_k(e^{-2\pi \frac{m}{M}})$, but $\psi_k[m] = \Psi_{0, k+1}(e^{-2\pi \frac{m}{M}})$ or $\varphi_k[m] = \varphi_{0, k+1}(e^{-2\pi \frac{m}{M}})$ can also be used. The related inverse transforms can be written in a similar form

$$f[n-m] \approx \frac{1}{g[m]} \sum_{k=0}^{N-1} \mathcal{R}_\phi \mathcal{F}_g f[n, k] \phi_k[m]. \quad (3)$$

This procedure can also be interpreted as a windowed Fourier transform, but now we are using a different basis. In addition, if $a_0 = 0$ then $\varphi_k[m] = \phi_k[m] = \epsilon_k[m]$ so we get back the ordinary DSTFT as a special case. We note that the \approx token was used in Eq. (3). The main reason behind that there are no proper inversion formulas for the these kinds of rational systems at the uniform discretization of the unit disc. On the other hand, a perfect reconstruction is also possible if we resample the original signal f at an appropriate nonuniform discrete grid. For further details we refer to the proof of Theorem 2 in [6].

As a consequence of the formulas in Eqs. (2) (3) and since these are orthogonal and biorthogonal projections onto the k dimensional subspaces of $H^2(\mathbb{D})$ the following statements hold

$$\sum_{k=0}^{M-1} (f[n-m] g[m])^2 = \sum_{k=0}^{M-1} \mathcal{R}_\psi \mathcal{F}_g f[n, k] \overline{\mathcal{R}_\phi \mathcal{F}_g f[n, k]},$$

$$\sum_{k=0}^{M-1} (f[n-m] g[m])^2 = \sum_{k=0}^{M-1} \left| \mathcal{R}_\phi \mathcal{F}_g f[n, k] \right|^2,$$

for the related nonuniform discretization [8, 9]. It can be interpreted as the Parseval's formula of this transformation. Hence, it means that the energy of the windowed and the transformed signal are equal, so we have the same property as in the case of ordinary DSTFT.

Now, the generalized rational DSTFT spectrogram can be easily computed for the functions $f \in H^2(\mathbb{D})$ by using Eq. (2). Unfortunately, most of the real signals are the elements of $L^2(\mathbb{D})$ instead of $H^2(\mathbb{D})$. Nevertheless, we can handle this issue by using the analytic representation of real signals. Namely, we should compute the function $F = f + i\mathcal{H}f$ where \mathcal{H} denotes the well-known Hilbert transformation. For instance the `hilbert` command can evaluate F in MATLAB and then the generalized rational DSTFT can be applied on F . Moreover, the coefficients and the expansions in Eqs. (2) (3) can be easily calculated by using the `biort_coeffs` and the `mt_coeffs` commands of the RAIT MATLAB toolbox [10].

4. FEATURE EXTRACTION USING RATIONAL DSTFT

4.1. Dataset

EEG database provided by University of Bonn [11] is used in this study. The EEG database consists of five sets (A-E). Each set contains 100 segments of single channel EEG with length of 23.6s selected from multi-channel EEGs. Sets A and B have been recorded using the standard international 10-20 system for surface EEG recording. Five healthy volunteers were participated in these tests with eyes open and eyes closed in (A) and (B), respectively. For sets C, D and E five epileptic patients were selected for presurgical evaluation of

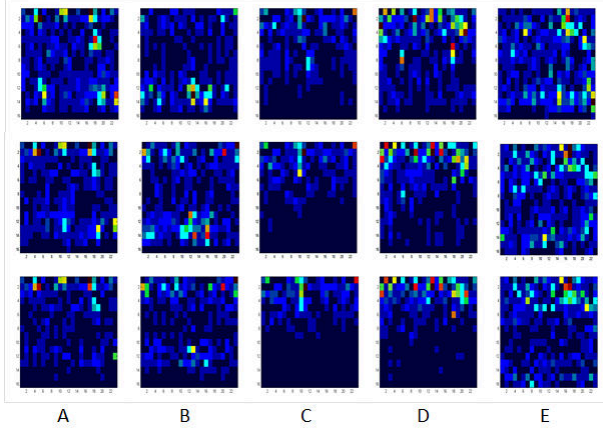


Fig. 1. Spectrogram of sets A to E for different selection of poles, First row) rational DSTFT spectra for pole $(0.1 + 0.1i)$, Second row) rational DSTFT spectra for pole $(-0.07 + 0.05i)$, third row) STFT spectra.

epilepsy patients using intracranial electrodes. In sets C and D, segments contain inter-ictal intervals while seizure activities occur in segments of set E. Each segment was sampled at 173.61 Hz resulting in 4096 samples.

4.2. Rational DSTFT coefficients

In the present work, we will apply the generalized rational DSTFT to EEG time-series. To comprise between compactness and time-frequency resolution, we represent each second of EEG time-series using 16 coefficients of MT rational DSTFT. To extract features from the rational DSTFT representation of the signal, we consider the absolute value of each coefficient. Furthermore, we add five statistical values to our feature vector which are extracted for each 1s long segment as follows: a) absolute mean value of coefficients; b) absolute median value of coefficients; c) absolute maximum value of coefficients; d) absolute minimum value of coefficients; e) absolute standard deviation value of coefficients. Hence, for each segment containing 1 second of the EEG time-series we obtain a feature vector with 21 feature elements. Fig. 1 shows the STFT and the rational DSTFT spectra for sets A, B, C, D and E by using two different poles. One can see that, as the pole tends closer to zero, the frequency response of rational DSTFT becomes more similar to the classical STFT.

5. CLASSIFICATION

To evaluate the efficiency and robustness of the proposed feature extraction method, we consider three different classification tasks. We mainly investigate seizure classification in the presence of seizure-free segments. The three classification tasks are: 1) classification of set E in the presence of set A (E - A); 2) classification of set E in the presence of sets A

and C (E - A, C); 3) classification of set E in the presence of sets A, B, C and D (E - A, B, C, D).

In all of these tasks we use Alternating Decision Trees (ADTrees) as the base classifier [12]. ADTrees are similar to option trees [13] which try to improve the boosting approach in order to achieve better classification result in comparison with a single tree.

5.1. Impact of the pole and the estimated coefficients

To analyze the impact of the position of the pole, we compare the classification results of the A-E problem for a set of poles chosen inside a 20×20 grid of the unit circle. We used 75% of each dataset as the training set and the remaining 25% as the test set. In this experiment, we extract MRF coefficients and use ADTree as the classifier. According to our experiments, by moving away from the center of the Cartesian grid (i.e., increasing the absolute value of the pole), there are some zero coefficients in the rational DSTFT. This phenomena is caused by the terms in Eq. (2) as they represent higher frequencies while the poles tend closer to the torus. These zero coefficients can reduce the accuracy of the A-E classification task up to 6%. However, we found that the classification accuracy is similar to STFT for the poles which are close enough to the center (i.e., $|a_0| \leq 0.07$). This can be seen on Fig. 2 where the classification results have been displayed at each pole. One can see that the classification results are similar near the zero pole. Moreover, we get exactly the same numbers for all property at the pole $(-0.1 + 0.1i)$. This behavior is a trivial consequence of the fact that the rational DSTFT is equal to the STFT for $a_0 = 0$. On the other hand, stepping away from zero can degrade the results by introducing more zero coefficients to the rational expansion. All the rational function systems defined in Section 2 share this property because they span the same subspaces of $H^2(\mathbb{D})$. For this reason, we decided not to fix the pole for the whole signal. More precisely, an optimal pole was chosen by using the well-known particle swarm optimization (PSO) algorithm [14, 15] to minimize the mean square error of the reconstructed signal. Taking advantage of this adaptive behavior of the rational function systems the error of the projection can be minimized. The purpose of the optimization procedure is to make a compact representation of each segment. Consequently, the coefficients can carry more information and they can be used as a feature. Precisely, the rational systems can be varied from segment to segment in contrast with the uniform representations such as STFT or even the Wavelets where the shapes of the base functions are fixed for all the segments. By this reason, we expect an improvement of the classification algorithms based on the classical STFT.

5.2. Bagged ADTree

In this section, we try to reduce the impact of the zero coefficients using ensemble learning. Though, ADTrees

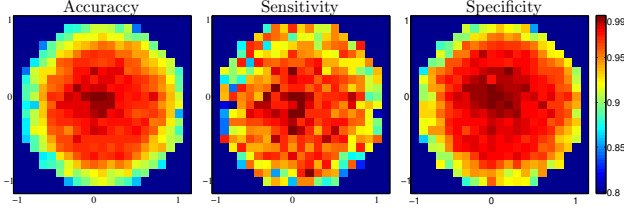


Fig. 2. Classification results according to each pole.

naturally perform a boosting ensemble learning algorithm, but here we also use bootstrap replicates to drawn different chunks from the original training set. The bagging is repeated k times to produce k bootstrap samples from the original one. At each time, the ADTree is trained with the k th bootstrap sample. A simple voting system at the end will decide which pattern indicates the majority of the results, then the voted pattern is chosen as the final class. In our work, the main idea of using bagging jointly with ADTrees is to make classification results independently from the value of the poles. It is a necessary step, because in each segment the optimal value of the pole is selected via a stochastic search using the hyperbolic modification of the basic PSO algorithm [16]. This procedure can affect the variance of the extracted coefficients which can cause instability in the classification results.

6. RESULTS

In this section, we compare the performance of different rational DSTFT systems with its competitive transform, STFT, in terms of classification accuracy. For all the three classification problems defined in Section 5, we consider 75% of the data, chosen randomly, as the training set and rest of the data as the test set. In addition, for STFT and all the rational DSTFTs, we extract a feature vector containing 21 elements (16 coefficients + 5 statistical values). Furthermore, the bagged ADTree is fixed with $k=20$ iterations during the comparison. Tab. 1, shows the classification accuracy for three classification problems. As it can be seen, the rational DSTFT system using MT coefficients yields the highest classification accuracy. For classification problem of sets E - A, both STFT and MT rational DSTFT achieve the same results. However, the MT coefficients outperform STFT coefficients in classification problems of E - A, C and E - A, B, C, D. In addition, the MRF representation results in better classification accuracy than the classical STFT in problem of E - A, B, C, D. For this classification problem the MT representation can outperform the STFT coefficients. The lowest classification accuracy in all the three classification problems is obtained by the biorthogonal rational function system. Furthermore, the inverse discrete (ID) STFT of the signal was computed by using 16 coefficients for each segment. Then the average mean square error was evaluated for all EEG records of the Bonn dataset. As it can be seen in Fig. 3, the overall MSE's

Table 1. Comparison of classification accuracies of different rational DSTFT coefficients and STFT coefficients.

Rational coefficients	Classification Problem		
	E-A	E-A, C	E-A, B, C, D
STFT	0.997	0.982	0.956
Biorthogonal	0.976	0.948	0.931
MT	0.997	0.986	0.967
MRF	0.991	0.973	0.963

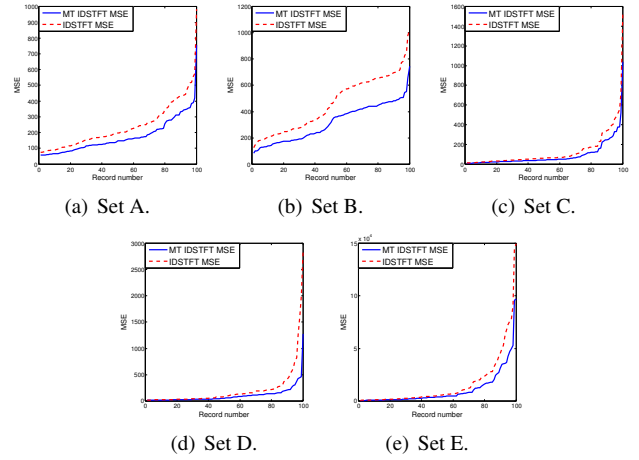


Fig. 3. Mean Square Errors for Bonn Database.

of the ordinary and MT IDSTFT are $2.23 \cdot 10^3$ and $3.47 \cdot 10^3$, so we achieved an improvement by 55% in this sense. As a consequence, our representation is more robust than the classical STFT. In other words, the proposed method provides a sparse representation of the signal while the components remain orthogonal (i.e., there is no redundancy).

7. CONCLUSION

In this paper, we propose the rational DSTFT and explore the efficiency of rational functions by describing the epileptic seizure patterns in time-frequency domain. The stochastic hyperbolic PSO search method is used to find the optimum value of the pole for each segment of EEG signals. Our method can provide an adaptive and scalable representation of the signal which can be competitive to the classical STFT in terms of feature extraction and MSE of the inverse transform.

In order to have a more scalable representation, we can use multi-dimensional (MD) PSO [15, 17] to find the optimum number of unique poles. MDPSO can search through multi-dimensional problem spaces and converges to the poles in the optimal dimension. Furthermore, by taking advantage of the adaptive behavior of the rational representations, we expect that our method can perform better on long-term EEG recordings as well. Hence, we are planning to prove this assumption in the future.

8. REFERENCES

- [1] L. Chen, E. Zhao, D. Wang, Z. Han, S. Zhang, and C. Xu, "Feature extraction of EEG signals from epilepsy patients based on Gabor transform and EMD decomposition," in *Proceedings of the 6th International Conference on Natural Computation (ICNC)*, 2010, vol. 3, pp. 1243–1247.
- [2] S. Nasehi and H. Pourghassem, "Real-time seizure detection based on EEG and ECG fused features using Gabor functions," in *Proceedings of the International Conference on Intelligent Computation and Bio-Medical Instrumentation (ICBIMI)*, 2011, pp. 204–207.
- [3] S. Fridli, L. Lócsi, and F. Schipp, "Rational function system in ECG processing," in *Computer Aided Systems Theory—EUROCAST 2011: Part I*, R. Moreno-Díaz et al., Ed., vol. 6927 of *LNCS*, pp. 88–95. Springer-Verlag Berlin, Heidelberg, Germany, 2011.
- [4] L. Lócsi and P. Kovács, "Processing ECG signals using rational function systems," in *Proceedings of the 7th IEEE International Symposium on Medical Measurements and Applications (MeMeA)*, 2012, pp. 1–5.
- [5] S. Fridli, P. Kovács, L. Lócsi, and F. Schipp, "Rational modeling of multi-lead QRS complexes in ECG signals," *Annales Univ. Sci. Budapest., Sect. Comp*, vol. 37, pp. 145–155, 2012.
- [6] S. Fridli and F. Schipp, "Biorthogonal systems to rational functions," *Annales Univ. Sci. Budapest., Sect. Comp*, vol. 35, pp. 95–105, 2011.
- [7] P. S. C. Heuberger, P. M. J. Van den Hof, and B. Wahlberg, *Modelling and Identification with Rational Orthogonal Basis Functions*, Springer-Verlag, London, UK, 2005.
- [8] L. Lócsi, "Calculating non-equidistant discretizations generated by blaschke products," *Acta Cybernetica*, vol. 20, pp. 111–123, 2011.
- [9] P. Kovács and V. Vad, "Fast computing of non-uniform sampling positions for real signals," in *Proceedings of the 15th International Symposium on Symbolic and Numeric Algorithms for Scientific Computing (SYNASC)*, 2013, (to appear).
- [10] P. Kovács and L. Lócsi, "RAIT: the rational approximation and interpolation toolbox for MATLAB," in *Proceedings of the 35th International Conference on Telecommunications and Signal Processing (TSP)*, 2012, pp. 671–677.
- [11] R. G. Andrzejak, K. Lehnertz, F. Mormann, C. Rieke, P. David, and C. E. Elger, "Indications of nonlinear deterministic and finite-dimensional structures in time series of brain electrical activity: Dependence on recording region and brain state," *Physical Review E*, vol. 64, no. 6, 1, 2001.
- [12] Y. Freund, "The alternating decision tree learning algorithm," in *Proceedings of the 16th International Conference on Machine Learning (ICML)*, 1999, pp. 124–133.
- [13] W. Buntine, "Learning classification trees," *Statistics and Computing*, vol. 2, pp. 63–73, 1992.
- [14] J. Kennedy and R. C. Eberhart, "Particle swarm optimization," in *Proceedings of IEEE International Conference on Neural Networks*, 1995, vol. 4, pp. 1942–1948.
- [15] S. Kiranyaz, T. Ince, and M. Gabbouj, *Multidimensional Particle Swarm Optimization for Machine Learning and Pattern Recognition*, Springer-Verlag Berlin, Heidelberg, Germany, 2014.
- [16] P. Kovács, S. Kiranyaz, and M. Gabbouj, "Hyperbolic particle swarm optimization with application in rational identification," in *Proceedings of the 21st European Signal Processing Conference (EUSIPCO)*, 2013, (to appear).
- [17] S. Kiranyaz, J. Pulkkinen, A. Yildirim, and M. Gabbouj, "Multi-dimensional particle swarm optimization in dynamic environments," *Expert Systems with Applications*, vol. 38, no. 3, pp. 2212–2223, 2011.